Solid Freeform Fabrication 2023: Proceedings of the 34th Annual International Solid Freeform Fabrication Symposium – An Additive Manufacturing Conference
Reviewed Paper

Analysis of Flow Additives in Laser-Based Powder Bed Fusion of Polymers: Implications for Flow Behavior, Processing, Temperature Profile, and Part Characteristics

S. Cholewa[a,b], A. Jaksch[b], D. Drummer[b]

[a] Collaborative Research Center - Additive Manufacturing (CRC 814), Friedrich-Alexander-Universität Erlangen-Nürnberg, Am Weichselgarten 10, 91058 Erlangen, Germany

[b] Institute of Polymer Technology (LKT), Friedrich-Alexander-Universität Erlangen-Nürnberg, Am Weichselgarten 10, 91058 Erlangen, Germany

Abstract

Powder bed fusion of polymers requires the use of flow additives to ensure adequate flowability of the feedstock material. However, information regarding flow additives and their load is limited, as is an understanding of their impact on processing conditions. This study investigates the flow behavior using static and dynamic measurements under process conditions, focusing on the influence of flow additives. Subsequently, processing studies are conducted using thermography to analyze the laser-material interaction. The characteristics of parts produced from Polypropylene and Polyamide 12 systems are also examined. The findings of this research enhance the understanding of the impact of flow additives on the processing conditions of laser-based powder bed fusion of polymers, potentially leading to optimized process parameters and improved part quality and mechanical properties.

Introduction

The term “Additive Manufacturing" (AM) refers to a wide range of technologies that all share a unique building method; it is a form of manufacturing where the three-dimensional (3D) product is often built into its designed shape using a layer-by-layer approach directly from a computer-aided design (CAD) model. This makes AM fundamentally different from conventional formative or subtractive methods because it is a tool-free process, and it has several independent units creating a significantly more significant degree of complexity in terms of cost-effectiveness [1].

The Laser-Based Powder Bed Fusion of Polymers (PBF-LB/P) method is widely recognized as one of the most general additive manufacturing processes employed for the fabrication of functional components, thanks to its favorable mechanical properties [2]. The polymer powder feedstock material is deposited onto a heated build platform using a powder spreading unit, such as a blade or a roller. After the powder has reached the defined build chamber temperature, exposure of the desired geometry is carried out by a laser, typically a CO_2 laser. The preheated powder melts and fuses together, resulting in a dense melt, while the non-irradiated powder acts as a support structure. This process is repeated until the build job is complete. The boundary conditions of the PBF-LB/P process necessitate specific feedstock material characteristics. In the context of PBF-LB/P, polymer properties have been categorized as intrinsic or extrinsic [3, 4]. Intrinsic characteristics include thermal, rheological, and optical properties. Extrinsic powder properties play a crucial role in achieving a homogeneous powder bed after powder application [5].

State of the Art

Each laser-based powder bed fusion cycle begins by applying a powder layer to the build area. Consequently, the powder properties have a key role in the process [6]. Several studies conclude that a homogeneous powder bed before fusion is necessary to reduce the void spaces between the particles filled during

coalescence to achieve a fully dense part with desired mechanical properties and sufficient surface quality [7, 8]. The density of the powder layer is closely related to the density of produced parts, as shown by Schmid et al. [9]. The flow behavior is influenced by various powder properties, including particle size distribution (PSD). Dechet et al. [10] compared different particle sizes of PA11 by sieving, followed by dry coating with 0.5 wt% hydrophobic fumed silica, and concluded that PSD narrowing and fumed silica coating could significantly improve the flowability of the PA11 powder. In another study by Schmidt et al. [11], a process chain that includes wet grinding, followed by a rounding process in a downer reactor, and a dry coating step was developed for Polystyrene. The flowability of the polymer powders significantly improved after rounding and dry coating, as demonstrated by reduced tensile strength.

Dadbaksh et al. [12] used fine-powder thermoplastic polyurethane (TPU) with flow additives in comparison with coarse powders and showed an increase in processing temperature and in part density. Ziegelmeier et al. [8] investigated the influence of bulk behavior and flowability on the final part properties and concluded that the surface roughness and mechanical performance of the manufactured parts depend on the powder density and surface quality. In addition, improving the density and flowability of the powder had a positive effect on reducing porosity and pore volume.

It is standard to dry coat the particles with flow additives to generate a good flow behavior which leads to a dense powder bed. Dry powder coating involves the creation of surface-functionalized composite particles by combining host particles with nanoscale guest particles. The composite particles are formed through the adhesion of nanoparticles onto the host particles, introducing roughness. This results in a considerable reduction of Van der Waals interaction forces between particles, consequently enhancing flowability [13]. It is demonstrated that there is an optimum range of flow aid concentration where flowability is maximized, and below a certain level, flowability is not significantly improved. The addition of further amounts of additives leads to a noticeable improvement, but there is a critical limit at which the positive effect diminishes [14, 15]. In addition to that optimum range, Kleijnen et al. [16] observed a delayed coalescence of the particles via hot stage microscopy. Nevertheless, there are only a few studies that look at the influences of the entire process and show which interactions occur.

In addition, there is a fundamental challenge in the existing evaluation of the flow properties of powders destined for the PBF-LP/P. While several techniques exist for measuring powder flow, the flowability of a powder is highly dependent on the nature of the applied flow field, and virtually none of the available techniques exhibit the boundary conditions of the process [6, 17]. Van den Eynde et al. [17, 18] therefore reproduced an application system on a laboratory scale that simulates the application; these experiments lead to the determination of the weight of the applied layer and thus the packing density was calculated. Additionally, the influence depending on the geometry as well as the particle shape was observed. Unfortunately, there are no further studies with this setup that take into account process variables such as coating thickness, temperature, application speeds, etc.

Therefore, this paper presents a new setup that mimics powder application in a PBF-LP/P machine, and provides a proper evaluation of the powder flowability for this process via surface measurements of the powder bed. Furthermore, with this equipment, different powders with different additive content are investigated, subsequently processed, and examined by means of a thermocamera to investigate influences on the process in more detail. Finally, component properties are evaluated by means of density.

Experimental Procedures

To investigate the effect of the different flow aids and loads on the processing and component properties, two types of additives were added separately and together to an isotactic homo Polypropylene (PP) from LyondellBasell and a Polyamid12 (PA12) from Evonik feedstock materials. Both materials were cryogenically ground, and the flow additives were added in concentrations of 0.05 wt.% and 0.1 wt.% and dry-mixed using a shaker at 49 rpm [19]. The additives utilized in PBF/LB-P have a dual purpose. Firstly, they function as distance-increasing agents to reduce particle adhesion, thereby enhancing the flowability of the powder (SiO_2, D17, Evonik). This property helps to mitigate any potential clumping or agglomeration issues during the powder bed fusion/layer-by-layer processing. Additionally, the inclusion of pyrogenic alumina (Al_2O_3, AluC, Evonik) in the additives serves to prevent the accumulation of electromagnetic charge, which could otherwise result in inadequate powder application. By minimizing electrostatic effects, the pyrogenic alumina promotes a more controlled and uniform distribution of the powder during the printing process. Both additives are from Evonik. Table 1 displays the different composite materials for PP and PA12 used in this work.

Table 1: Material combinations used in this study

Mixture number	***Al_2O_3 in wt.%***	***SiO_2 in wt.%***
1	Ø	Ø
2	Ø	0.05
3	Ø	0.1
4	0.05	Ø
5	0.05	0.05
6	0.05	0.1
7	0.1	Ø
8	0.1	0.05
9	0.1	0.1

Particle Shape and Particle Size Distribution

For the investigation of particle size and shape of the used flow additives, scanning electron microscope (SEM) images with the Ultra Puls from Carl Zeiss AG were conducted. The images of the gold sputtered powders were recorded at a magnification of 500 and 2000 and an acceleration voltage of 5 kV. The Mastersizer 2000, equipped with a Scirocco 2000 dry dispersing unit from Malvern Panalytical, was employed for laser diffraction particle sizing to determine the particle size distribution (PSD). The dispersing unit was operated at a pressure of 2 bar, and the feed rate was set to approximately 50% [20].

Powder Flowability

A reliable method for evaluating the powder flow properties is the compaction depth, as described by Hesse et al. [21]. This characteristic value, which is highly reproducible, provides valuable insights into the static properties of the powder [21, 22]. Powder flowability investigations were performed on a Discovery HR-2 rheometer (TA Instruments). The setup consists of an upper 25 mm plate parallel to a container with an inner diameter of 27 mm. The powder was sieved loose and unpacked into the container. To establish a defined baseline, which results in better comparability, a normal force of 0.2 N was applied to the bulk powder. Afterward, the upper parallel plate was moved with a constant compression rate of 1 µm/s into the powder bed, and the normal force was observed. The experiments were conducted at room temperature (22 °C). For a qualitative comparison of the systems in addition to the force progression, the distance passed for a defined force difference (from 0.2 to 2.5 N) was used.

Powder Application System

As in the state of the art, the challenge with many measurement methods is the transfer to the process, since many measurement methods are also carried out statically or under high loads, such as the shear cell, which only conditionally correspond to the boundary conditions of the process. Therefore, this paper presents a set-up in Figure 1 that reflects the boundary conditions in the process. Ultimately, it is the construction of a PBF-LP/P

machine, but instead of the laser irradiation, it has a 3D scanner (structured light projection - fringe projection) that records the powder surface for analysis. The powder is supplied by the feeder tank, which can provide various defined quantities, followed by the recoater, which applies the powder to the free adjustable build chamber. Various application systems (roller, various blade geometries) are tested here. The speed of the application is also freely defined. In addition, the feed chamber, the build chamber and the powder surface temperature can be adjusted. For the powder surface, a pyrometer is used as in the process, and the irradiation is carried out by an infrared heater. Both chambers have thermocouples for temperature control. In addition, the powder chamber is also flushed with nitrogen. In this study, the different materials with additive content were investigated with a blade, an application speed of 150 mm/s, and a layer thickness of 120 µmm. For this purpose, 5 repetitions were carried out at room temperature. For comparison, the different systems' surface roughness with areas of 35 mm x 35 mm were compared with each other. The analysis was carried out with a MountainsMap from Digital Surf.

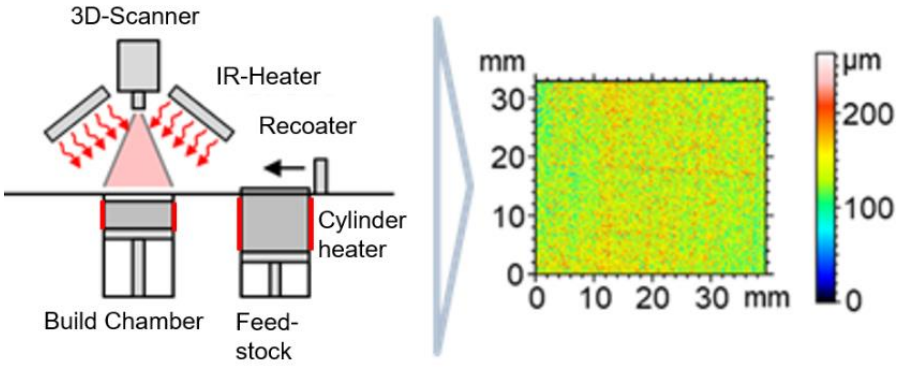

Figure 1: Schematic illustration of the powder application system setup

Thermal Investigations

To determine whether the additives have an influence on the thermal properties, and in particular whether they act as nucleation nuclei to increase the crystallization temperature and accelerate the crystallization process, thermal investigations were carried out with differential scanning calorimetry (DSC) measurements. The polymer (2−5 mg) was sealed into a DSC aluminum pan and heated from 0 to 200 °C and 220 °C for PP and PA12 respectively at 10 K/min^{-1}. After maintaining the temperature for 5 minutes to delete the thermal history, the sample was cooled to 0 °C at rates of 10 K/min^{-1} and then reheated using the same procedure. The reported values for the process window were obtained from the first heating and cooling cycle. For isothermal measurements, an identical heating procedure was employed. Subsequently, the samples were cooled down to the desired isothermal holding temperatures of 136 °C and 166 °C for PP and PA12 respectively at a cooling rate of 60 K·min^{-1}. The progress of crystallization was assessed based on the crystallization half-time, which denotes the time taken for 50% of the crystallization process to occur.

Processing

The processing experiments were carried out on a research system described by Greiner et al. [23]. The systems building space was 350 × 350 mm^2. The machine was equipped with a 30 W CO_2 laser with a focus diameter of 0.4 mm. For the conducted experiments, an inlet (100 × 100 mm^2) was used to enable builds with small powder quantity. The powder coating was executed with a blade and a recoating speed of 150 mm/s.
To define the process parameters, a full factorial study at three levels for single layers with 10 mm x 10 mm was performed. Therefore, the process parameters laser power (P_L), hatch distance (hs), and scan speed (vs) were changed with three factors. Thereby, energy densities E_D from 8 mJ/mm² to 100 mJ/mm² were covered (see Table 2). Furthermore, for PP and PA12 the building temperatures were set to 155 °C and 172 °C, respectively.

$$E_D = \frac{P_L}{v_s\, h_s} \qquad (1)$$

Table 2: Parameter study for single layers with according running number (1-27, light grey). The values are the energy density in mJ/mm².

vs	2000 mm/s						1500 mm/s						1000 mm/s					
hs / P	0.3 mm		0.2 mm		0.1 mm		0.3 mm		0.2 mm		0.1 mm		0.3 mm		0.2 mm		0.1 mm	
5 W	1	8	2	13	3	25	4	11	5	17	6	33	19	17	20	25	21	50
7.5 W	7	13	8	19	9	38	10	17	11	25	12	50	25	25	26	38	27	75
10 W	13	17	14	25	15	50	16	22	17	33	18	67	22	33	23	50	24	100

The best process parameter set was defined when the target values in Minitab were set to reach the determined area of 100 mm², the ratio of length to width was 1, and the lowest porosity for each single layer was obtained. All these values were obtained by optical analyses using OpenCV python. An energy density of 33 mJ/mm² (set 17) was selected for PA12, and an energy density of 22 mJ/mm² (set 22) for PP.

Thermal Investigations

An infrared (IR) thermographic system Velox 1310 k SM (IRCAM GmbH, Erlangen, Germany) was applied for characterizing the powder laser interaction. The system functions within the short and medium wavelength spectrums, specifically ranging from 1.5 to 5.5 µm. Greiner et al. [23] provide a schematic depiction of the assembly configuration. To safeguard the indium antimonide (InSb) detector, a sapphire glass window was positioned in front of the IR camera. The sapphire glass is not transparent to radiation of wavelengths above 6 µm, thereby filtering out the CO_2 laser wavelength (λ_{CO2} = 10.6 µm). The frame rate was set to 150 Hz, with a pixel size of 100 x 100 µm. In all experiments, a simplifying assumption was employed to maintain a constant emission coefficient and adjust it based on the initial temperature of the build chamber; this was determined using the system's pyrometer. This approach attempts to investigate whether different packing densities due to different flow aids as well as the flow aids themselves have a direct influence on the laser material interaction. Here, two factors are taken into account: the maximum temperature reached during exposure to each parameter, and the average temperature experienced throughout the exposure.

Part Density

To determine the density of the samples and gain insights into their porosity, Archimedes measurements were performed [24]. The technique relies on the principle of Archimedes, where the volume of liquid displaced is equivalent to the immersed volume of the sample. This principle enables the determination of sample volume and density. The samples were weighed both in air and in a liquid medium.

Results and Discussion

Powder Shape

Figure 2 shows SEM images of the PP pure and dry blended with flow aids. The particles display an edged surface which is explained by the powder manufacturing of cryogenic grinding. As seen with further magnification, the flow additives are homogeneously distributed on the host particle. The particle size distributions of the grinded powders are depicted as the numeric weighted cumulative sum distribution $Q_0(x)$ and the numeric density distribution weighted numeric $q_0(x)$ in Figure 2c. The particle size distribution is 83 µm and 88 µm for PA12 and PP respectively. Overall the particle size distribution of the two systems is similar with a higher fines content for the PA12.

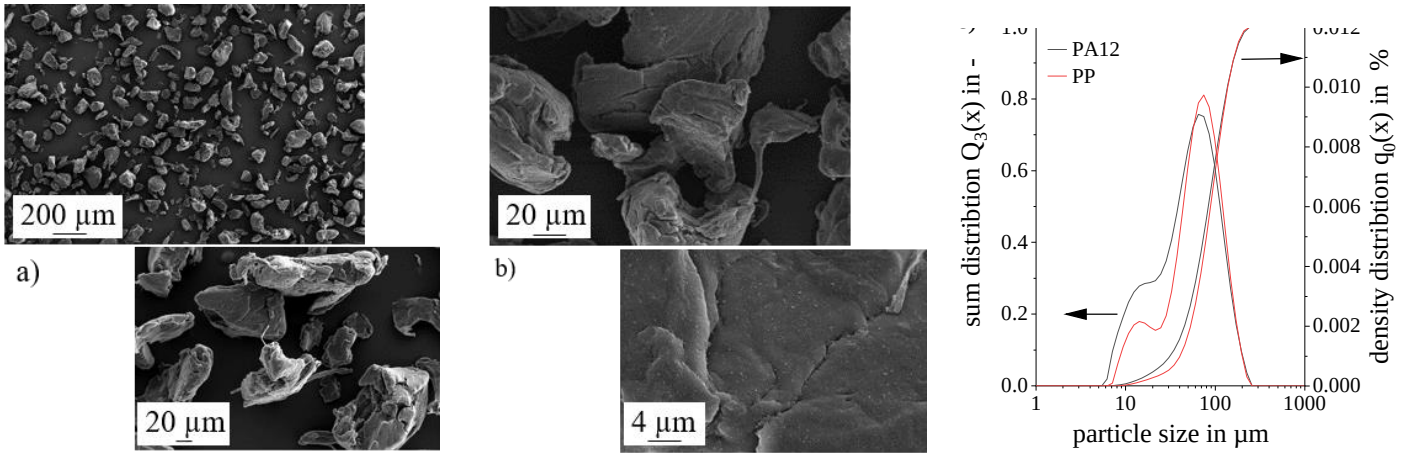

Figure 2: SEM images of the grinded PP, without flow aids (a) with flow aids 0.1 wt.% Al_2O_3 and SiO_2 (b), and the numeric weighed sum distribution and numeric density distribution of the PP and PA12 powder (c)

Powder Flowability

Compression Depths

Figure 3a illustrates schematically the development of normal force during uniaxial loading in the powder bed, comparing pure PP with PP containing flow additives. The relative change in height is measured based on the depth of the indenter as it applies a constant compression rate of 1 µm/s to a loosely consolidated powder bed with an initial normal force of 0.2 N. When examining the change in height, it is observed that the unadded PP requires slightly increased normal forces. On the other hand, the PP with additives necessitates higher forces for the same height changes. This disparity is attributed to the fact that the powder coated with flow additives possesses a greater powder bulk density compared to the pure powder. Consequently, a greater normal force is required to achieve the same level of height change. For an assessment of the influence of the different systems as well as possible interactions, an overview is given in Figure 3b and c, where the compression depth is given for the force differentials from 0.2 N to 2.5 N.

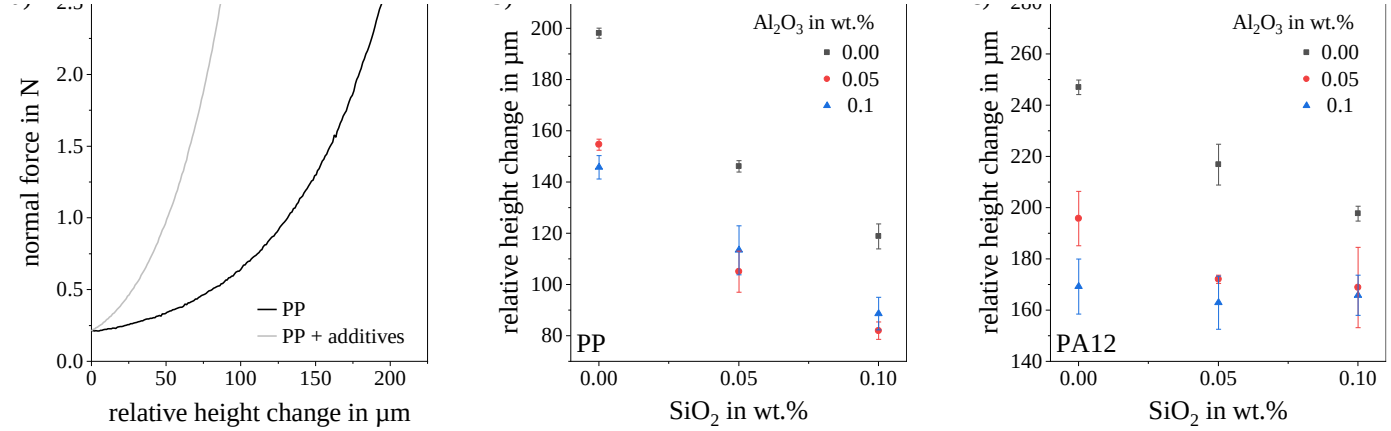

Figure 3: Schematic illustration of rise of normal force during a constant compression rate of the pure PP and dry-coated PP (a), relative height change for comparison for PP (b) and PA12 (c) with n = 5

If the main effects are considered independently of each other, the SiO_2 has a greater influence on PP. However, the Al_2O_3 reduces not only the electric charge but also the Van der Waals forces of the particles leading to a reduced compression depth. Moreover, it is found that a stepwise increase from 0.05 to 0.1 wt.% has only a small effect, indicating that further additions beyond this point have no significant effect, this is especially true for PP. While observing the interaction between the two additives, a comparable behavior is seen, with a minimum height change reached at 0.05 Al_2O_3 together with 0.05 wt.% and 0.1 wt.% SiO_2, with no further improvement as the Al_2O_3 content is increased.

In the case of PA12, the impact of Al_2O_3 is particularly intriguing as it surpasses the effect on compressibility observed in PP and holds a stronger influence than SiO_2. However, when the concentration is further increased to 0.1 wt.%, the improvement becomes less pronounced. When examining the combination of both additives, it is evident that there is no significant enhancement when transitioning from 0.05 wt.% of either component to a higher concentration blend, regardless of the proportions.

Powder Flowability

There is a noticeable difference amongst all compounds when comparing the compression depth of PP and PA12. This finding is supported by the application system's results, which consistently demonstrate that PP has a significantly lower surface roughness than PA12. This discrepancy implies a higher degree of homogeneity in the surface characteristics of the powder bed. It is evident that increasing the Al_2O_3 content alone to 0.1 wt.% is not an improvement, even when considering the interaction with SiO_2 blends. For PP, this leads to an optimum coating of 0.1 SiO_2 and 0.5 wt.% Al_2O_3.

If the additives are first examined separately for PA12, comparable effects like the compaction depth are also noticed here, where only a marginal improvement with further increase is detected. Even more intensively than for the compaction depth, it is shown that a further increase of SiO_2 in combination with Al_2O_3 leads to a deterioration of the powder surface.

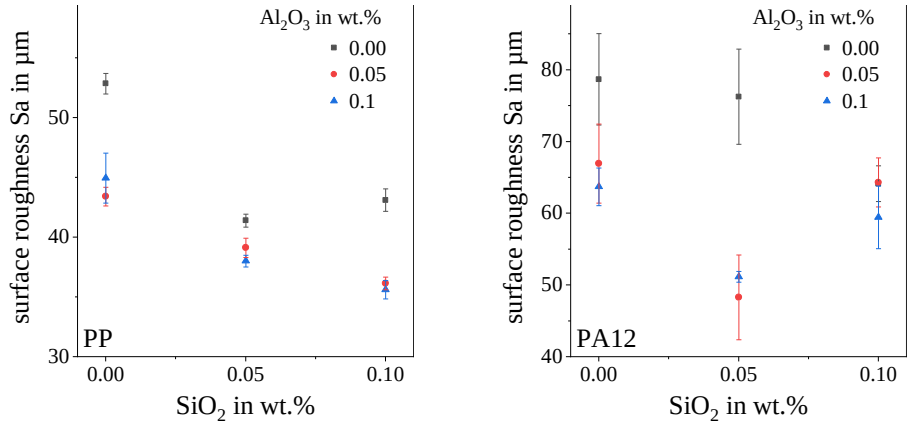

Figure 4: Surface roughness depending of different additive content for PP (a) and PA12 (b) with powder flowability set up (n = 5)

Thermal Investigations

The thermal characteristics of a polymer play a crucial role in determining the process parameters and overall process suitability. Throughout this temperature range, the molten material and the surrounding solid powder coexist. To ensure an adequate process window, the crystallization temperature of the polymer must be significantly lower than its melting temperature. This difference, known as the onset temperatures of crystallization and melting, is crucial. Ideally, polymers with a wide process window are preferred as they are less sensitive to temperature variations during the process, resulting in increased process robustness. Therefore, it is essential that additives do not act as nuclei and decrease this process window.

Figure 5a-c illustrates the dynamic thermogram, which captures the first heating and cooling cycle as well as the isothermal crystallization periods of the powder for 0.1 wt.% Al_2O_3 and SiO_2 respectively. When subjected to a heating and cooling rate of 10 K/min, the dynamic measurement revealed melting peaks at 178 °C / 164 °C, and a crystallization point at approximately 154 °C / 119 °C for PA12 and PP systems. Although not all measurements are illustrated in the graph for readability purposes, the results were seen for all possible

combinations. No influence of the additives compared to the pure material is detected with the measurement program carried out, but it is important to note that the selected cooling rate is considered overly high for the process. During the generation of layered components, it is important to maintain a quasi-isothermal process for a certain time period between the melting and crystallization temperatures.

Therefore, Figure 5c shows isothermal measurements that are more representative of the process and also more sensitive to changes. In general, the same statement applies for the dynamic measurements, and no significant difference is seen. Considering the typical partial crystallization time $t_{1/2}$, there is almost no difference between the high additive powders and the uncoated powder (having less than a 30 s difference). It is concluded that these two additives do not show any nucleation effect for the PP and the PA12.

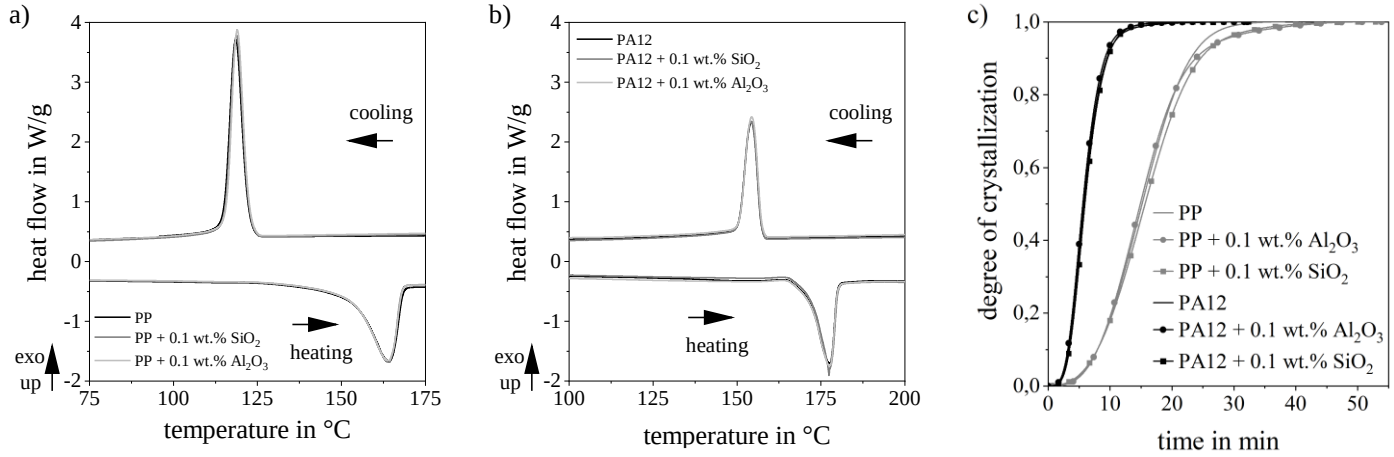

Figure 5: Dynamic DSC measurements with 10 K/min for PP with and without flow additives (a) and PA12 (b), isothermal crystallization at 166 °C for PA12 and 134 °C for PP (c)

Infrared Investigations

Figure 6a shows the thermal image after exposure for the material combinations of PA12. More details are given in Figures 6b and 6c, which show the maximum temperature and the mean temperature material peak for each material. The differences in the measured temperatures are dependent on the material systems, and amount to only a few °C which is not classified as relevant. A variation of the parameters at the same energy density leads to a much more pronounced change compared to the additive influence [25].

These results and findings are also observed for PP, hence why the influence of the additives on the measured temperature is considered negligible.

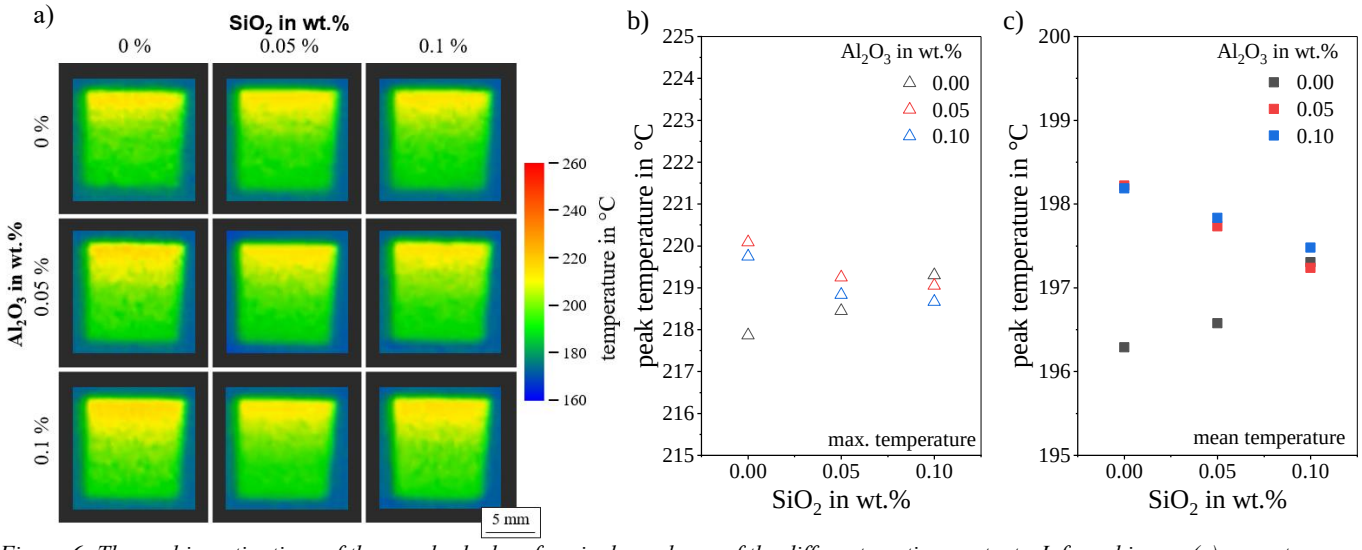

Figure 6: Thermal investigations of the powder bed surface in dependence of the different coating contents, Infrared image (a), max. temperature reached (b), and mean temperature (c) for PA12

Component Density

Figure 7 shows the measured component densities of the two material systems and their additive combinations with the same processing parameters for PP and PA12. The dependence of component densities in both PP and PA12 on the additive content of the starting powder is evident. In the case of PP, there is an increase in component density from 0.86 to 0.88 g/cm³. PA12 also exhibits an increase in component density from 0.98 to 0.99 g/cm³. Similarly to the flow analysis, it is seen that for both materials, a significant increase in the individual flow additives yields only a minor increase in density.

For both PP and PA12, it is observed that increasing SiO_2 to 0.05 leads to a rise in density, but it has little effect when increased past the stated range. Additionally, a reduction in the standard deviation is observed for the powders with additives. The observed differences in component density are attributed to a decrease in bulk density and an associated increase in the initial pore diameter.

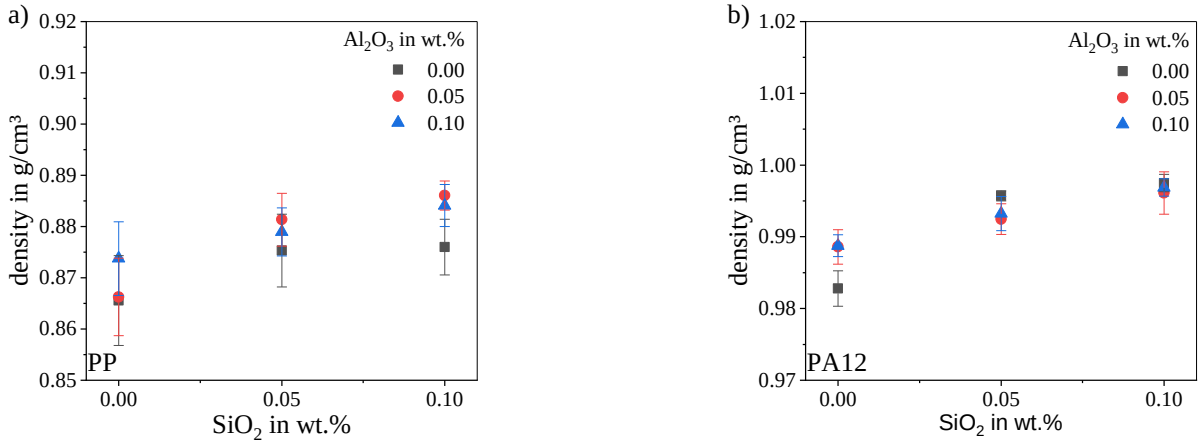

Figure 7: Density via Archimedes measurements for PP (a) and PA12 (b)

Summary and Outlook

In this study, the impact of different additives and loads on PP and PA12 were investigated for flowability, thermal properties, laser material interaction, and part density. Flowability studies were conducted with compression depths to reveal that a further increasing of additives does not lead to significant improvements. To compare these lab values, a new experimental set up was introduced which is able to mimic the process as close as possible. These measurements showed similar trends. It is shown that the Al_2O_3 improves the bulk density, and that best results are gained when both systems are added. Thermal investigations by means of dynamic and isothermal measurements showed no significant impact of the chosen systems to determine that a recoating of used powder with additives is possible since no earlier crystallization is expected. During processing, the laser material interactions was observed by Infrared thermography to investigate the different packing densities due to different flow aids and to study the flow aids themselves and if they have a direct influence on the process. The results indicate a neglect able impact on the temperatures. As expected the part density showed a strong dependence of the additives. However, like the flowability studies, further increasing of the share does not lead to denser part. Additional important influences to examine subsequently are the surface roughness and the mechanics of the components. To study the transfer of flow properties in more detail, it is necessary to increase the temperature in subsequent studies, and to take into account other influences such as velocity or layer thickness.

Acknowledgement

This study is funded within the IGF project (21598 N) with the title "Improving the aging stability of plastic powders for selective laser sintering by tailor-made additive systems" and by the Deutsche Forschungsgemeinschaft (DFG, German Research Foundation) – Project-ID 61375930 – SFB 814, sub-project

T10. The authors would like to thank Florentin Tischer of the Institute of Particle Technology at the FAU Erlangen-Nürnberg for providing particle size distribution data.

References

1. Ligon, S.C., et al., *Polymers for 3D Printing and Customized Additive Manufacturing.* Chem Rev, 2017. **117**(15): p. 10212-10290.
2. Wörz, A., et al., *Comparison of long-term properties of laser sintered and injection molded polyamide 12 parts.* Journal of Polymer Engineering, 2018. **38**(6): p. 573-582.
3. Schmid, M., A. Amado, and K. Wegener, *Polymer powders for selective laser sintering (SLS)*, in *AIP Conference Proceedings 1664*. 2015.
4. Chatham, C.A., T.E. Long, and C.B. Williams, *A review of the process physics and material screening methods for polymer powder bed fusion additive manufacturing.* Progress in Polymer Science, 2019. **93**: p. 68-95.
5. Dechet, M.A., et al., *A novel, precipitated polybutylene terephthalate feedstock material for powder bed fusion of polymers (PBF): Material development and initial PBF processability.* Materials & Design, 2021. **197**.
6. Schmidt, J. and W. Peukert, *Dry powder coating in additive manufacturing.* Frontiers in Chemical Engineering, 2022. **4**.
7. Wudy, K., *Alterungsverhalten von Polyamid12 beim selektiven Lasersintern*. 2017, FAU Erlangen-Nürnberg.
8. Ziegelmeier, S., et al., *An experimental study into the effects of bulk and flow behaviour of laser sintering polymer powders on resulting part properties.* Journal of Materials Processing Technology, 2015. **215**: p. 239-250.
9. Schmid, M., et al., *Influence of the Origin of Polyamide 12 Powder on the Laser Sintering Process and Laser Sintered Parts.* Applied Sciences, 2017. **7**(5).
10. Dechet, M.A., et al., *Production of polyamide 11 microparticles for Additive Manufacturing by liquid-liquid phase separation and precipitation.* Chemical Engineering Science, 2019. **197**: p. 11-25.
11. Schmidt, J., et al., *A novel process route for the production of spherical LBM polymer powders with small size and good flowability.* Powder Technology, 2014. **261**: p. 78-86.
12. Dadbakhsh, S., et al., *Effect of Powder Size and Shape on the SLS Processability and Mechanical Properties of a TPU Elastomer.* Physics Procedia, 2016. **83**: p. 971-980.
13. Zhou, H., M. Götzinger, and W. Peukert, *The influence of particle charge and roughness on particle–substrate adhesion.* Powder Technology, 2003. **135**: p. 82-91.
14. Laumer, T., et al., *Analysis of the Influence of Different Flowability on Part Characteristics Regarding the Simultaneous Laser Beam Melting of Polymers.* Physics Procedia, 2016. **83**: p. 937-946.
15. Tomas, J. and S. Kleinschmidt, *Improvement of flowability of fine cohesive powders by flow additives.* Chemical Engineering & Technology: Industrial Chemistry-Plant Equipment-Process Engineering-Biotechnology, 2009. **32**(10): p. 1470-1483.
16. R.G. Kleijnen, M. Schmid, and K. Wegener. *IMPACT OF FLOW AID ON THE FLOWABILITY AND COALESCENCE OF POLYMER LASER SINTERING POWDER* in *Proceedings of the 30th Annual International Solid Freeform Fabrication Symposium* 2019. Austin: Solid Freeform Fabrication.
17. Van den Eynde, M., L. Verbelen, and P. Van Puyvelde, *Assessing polymer powder flow for the application of laser sintering.* Powder Technology, 2015. **286**: p. 151-155.
18. Van den Eynde, M., L. Verbelen, and P. Van Puyvelde, *Influence of temperature on the flowability of polymer powders in laser sintering*. 2017.
19. Dusenberg, B., et al., *Enhancing Photoelectric Powder Deposition of Polymers by Charge Control Substances.* Polymers (Basel), 2022. **14**(7).
20. Tischer, F., et al., *Polyamide 11 nanocomposite feedstocks for powder bed fusion via liquid-liquid phase separation and crystallization.* Powder Technology, 2023. **424**.
21. Hesse, N., et al., *Towards a generally applicable methodology for the characterization of particle properties relevant to processing in powder bed fusion of polymers – From single particle to bulk solid behavior.* Additive Manufacturing, 2021. **41**.
22. Cholewa, S., et al., *Tailored Syndiotactic Polypropylene Feedstock Material for Laser-Based Powder Bed Fusion of Polymers: Material Development and Processability.* ACS Applied Polymer Materials, 2023. **5**(4): p. 2430-2439.
23. Greiner, S., et al., *Thermographic investigation of laser-induced temperature fields in selective laser beam melting of polymers.* Optics & Laser Technology, 2019. **109**: p. 569-576.
24. *DIN EN ISO 1183-1:2019-09.*
25. Greiner, S., et al., *Development of material-adapted processing strategies for laser sintering of polyamide 12.* Advanced Industrial and Engineering Polymer Research, 2021. **4**(4): p. 251-263.